energies

MDPI

Article

Numerical Simulation of Combustion and Characteristics of Fly Ash and Slag in a "V-type" Waste Incinerator

Zixue Luo [1,*], Wei Chen [1], Yue Wang [1], Qiang Cheng [1], Xiaohua Yuan [2], Zhigang Li [2] and Junjie Yang [2]

1 State Key Laboratory of Coal Combustion, Huazhong University of Science and Technology, Wuhan 430074, China; m201971231@hust.edu.cn (W.C.); m202171305@hust.edu.cn (Y.W.); chengqiang@hust.edu.cn (Q.C.)
2 Grandblue Environment Co., Ltd., Foshan 528200, China; yuanxiaohua@grandblue.cn (X.Y.); lizhigang3@grandblue.cn (Z.L.); yangjunjie1@grandblue.cn (J.Y.)
* Correspondence: luozixue@hust.edu.cn; Tel.: +86-27-8754-2417; Fax: +86-27-8754-5526

Abstract: This study is focused on a "V-type" waste incinerator for municipal solid waste (MSW) combustion. Computational fluid dynamics (CFD) methods are used to study the MSW combustion process. The characteristics of fly ash and slag are analyzed by using a laser particle analyzer, scanning electron microscope, X-ray fluorescence, and X-ray diffraction. The results show that the error between the CFD simulation data and measured data is less than 10%, and the changing trend of the combustion process is well-modeled. The fly ash mainly has an irregular spherical or ellipsoid structure, whereas the slag mainly has an irregular porous structure. The main constituents of the ash and slag are CaO and SiO_2, along with heavy metal elements such as Cu, Pb, and Cr.

Keywords: waste incinerator; numerical simulation; fly ash; slag

check for updates

Citation: Luo, Z.; Chen, W.; Wang, Y.; Cheng, Q.; Yuan, X.; Li, Z.; Yang, J. Numerical Simulation of Combustion and Characteristics of Fly Ash and Slag in a "V-type" Waste Incinerator. *Energies* **2021**, *14*, 7518. https://doi.org/10.3390/en14227518

Academic Editor: Elena Magaril

Received: 19 October 2021
Accepted: 9 November 2021
Published: 11 November 2021

1. Introduction

With the growth of the population, economic development and urban expansion year by year, the amount of generated municipal solid waste is also increasing [1]. Traditional landfill methods are facing numerous challenges such as land restrictions and pollution, and how to deal with millions of tonnes of household waste is becoming the biggest problem facing environmental managers [2,3]. Waste incineration has become one of China's main waste disposal methods because of its advantages of waste reduction, resource availability, and safety [4]. However, the pollutant emission standards for municipal solid waste (MSW) incinerators are becoming increasingly stringent. In 2016, the Chinese government also included domestic waste fly ash in the national list of hazardous waste. The National Standard for Environmental Protection of the People's Republic of China (HJ 1134-2020) published in August 2020 will prevent environmental pollution, improve ecological quality and regulate and guide the environmental management of household waste incineration fly ash [5,6]. Accordingly, more advanced technologies must be adopted in the waste incinerators.

At present, the common grates mainly include Mitsubishi-Martin type, Keppel Seghers type, Hitachi Shipbuilding type and so on. In order to realize the effective treatment of existing urban domestic garbage and the building of a "waste-free city", a new type of "V-type " grate has appeared. Compared with the traditional Martin-type reverse push grate, the grate structure adopts a special V-shaped layout, as shown in Figure 1a. The V-type grate combines the action of inverse tilt forward push and inverse tilt gravity, so as to achieve good tumbling and mixing. As shown in Figure 1b, due to the structural characteristics of the V-type grate, the materials burn more fully, the heat loss of chemical incomplete combustion and mechanical incomplete combustion is reduced, and the thermal efficiency of the boiler is improved. The adaptability of the incinerator to the incoming materials has also been strengthened, which is conducive to the uniform and stable incineration of multi-source organic solid waste. The internal gas recirculation system (IGRS) is the latest low air ratio combustion technology used in waste-to-energy projects. Flue gas with a higher oxygen content is extracted from the combustion zone and blown as secondary air to the secondary combustion zone, which brings the advantages of energy saving, high efficiency and reduced pollutant emissions.

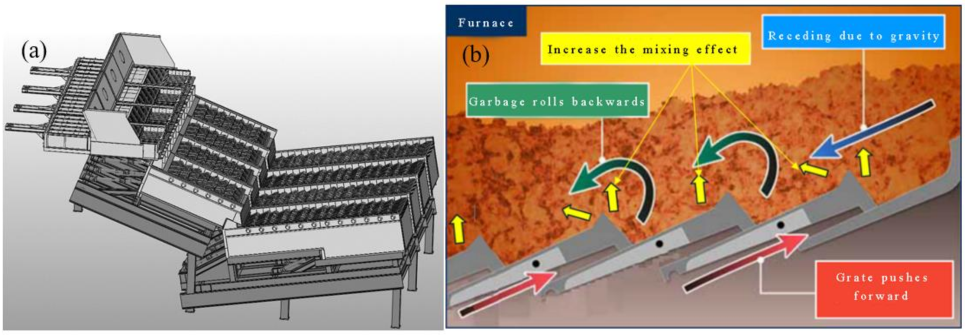

Figure 1. Structure schematic of a V-type grate: (**a**) Description of overview grate panel; (**b**) Description of operation condition.

Factors such as fuel characteristics and primary and secondary air distribution affect the combustion in the waste incinerator. Owing to the high cost of manpower and material resources in field experiments, a combination of simulations and experiments is usually used to study the waste incineration process. In recent years, computational fluid dynamics (CFD) has become a powerful tool for simulating waste incineration in furnaces. César A. et al. [7] and Karim, M.R. et al. [8] simulated the combustion process of waste incinerators by defining related subroutines in Fluent. Yang, Y.B. and Swithenbank, J. [9] systematically described the bed solid-phase combustion process and developed a bed simulation software, FLIC, to calculate bed solid fuel combustion. Yan et al. [10] performed an optimization simulation of the air preheating temperatures. Xu et al. [11] simulated waste sludge blending and found that with an increase in the mixing amounts of sludge, the solid-phase combustion process of the grate was delayed and the temperature decreased. Becidan, M. et al. [12] performed oxyfuel combustion experiments in a laboratory-scale reactor, showing that a model MSW can be satisfactorily combusted under different oxyfuel conditions provided that the oxygen concentration in the oxidizer is carefully adapted.

Another key issue regarding waste incineration is the generation and emission of pollutants. MSW produces dioxins and heavy metals during the combustion process and eventually accumulates in fly ash. Improper disposal of fly ash affects the environment [13,14]. A lack of understanding of the fundamental characteristics of fly ash affects the treatment of waste incineration fly ash. The characteristics of fly ash and slag were analyzed to provide a scientific basis for the effective disposal of waste incineration fly ash.

The main objective of this study is to use fluid dynamic incinerator code (FLIC) and Fluent to simulate the combustion process in the new V-type grate furnace and analyze the basic characteristics of MSW incineration ash and slag, so as to study the MSW incineration process in an all-round way and provide a certain theoretical reference for the comprehensive utilization of MSW.

2. Materials and Methods

2.1. Numerical Model

The simulation of the waste incineration process was divided into two parts: the simulation of the combustion of the solid phase in the bed and the simulation of the combustion of the gas phase in the incinerator [15]. The gas-phase temperature, concentration, and velocity of each component at the top of the bed were calculated using FLIC. FLIC was a simulation software for bed combustion reactions, which were mainly used for the simulation of laminar combustion of fuels with high moisture and high volatile matter such as biomass and waste. Fluent software can simulate flow, heat transfer and some chemical reactions. Users can adjust the parameters during setting according to specific requirements to make the simulation more in line with actual working conditions. The FLIC simulation results were imported into Fluent and used as the inlet boundary conditions for the gas-phase combustion simulation [16]. Then, the radiation flux of the bed was imported to the FLIC as the radiation boundary. The two processes were repeated until the results converged [17,18]. The solid-phase combustion reaction in the bed was simulated by using the FLIC software [19,20]. Owing to the non-uniformity of the grate's radiation intensity distribution, the grate was divided into eleven and five sections along the length and width, respectively. The corresponding radiation intensity was input into the FLIC. The radiation intensity distribution along the grate width was symmetrical, and only the solid-phase combustion of the wastes in the first, second, and third sections was evaluated. The bed segmentation process is shown in Figure 2. The non-uniformity distribution of the waste composition was ignored.

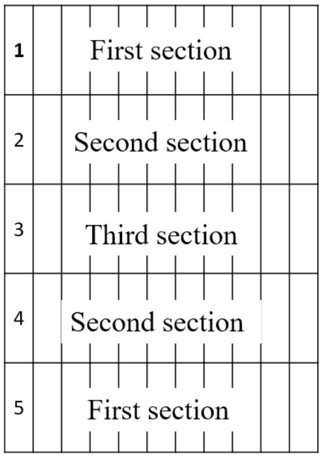

Figure 2. Waste incineration bed segmentation.

The furnace gas-phase combustion reaction was simulated by Fluent. The gravitational acceleration was set to 9.8 m/s^2. Turbulence was modelled by using the standard $K-\varepsilon$ two-equation model with a standard wall. The velocity inlet boundary conditions were adopted for the primary and secondary air inlet. The simulation results of FLIC were set as the primary air inlet boundary condition. The secondary air inlet velocity was 9.161 m/s, the temperature was 464.55 K, the mole fraction of O_2 was 0.21 and the mole fraction of N_2 was 0.79. The pressure outlet boundary condition was adopted for the flue gas outlet [21] with the outlet pressure at −60 Pa, and the total reflux temperature was 900 K. The P-1 model with a small calculation amount suitable for combustion equipment with complex geometric structures was adopted for the radiation modeling, and cooperated with the gray-gas mass weighted summation method to solve the absorption coefficient. '*PRESTO!*' was used for pressure discretization [22]. The '*simple*' algorithm was used for pressure-velocity coupling, the furnace wall was set as an adiabatic boundary condition, and the water-cooled wall was treated under the condition of approximately constant wall temperature. The finite rate/vortex dissipation model was used for gas phase combustion. Based on elemental conservation and energy conservation, the gas-phase products of waste incineration were simplified to CH_4, CO, H_2, CO_2 and H_2O [23,24]. The following simplified reactions were used in the gas-phase combustion.

$$CH_4 + 1.5O_2 \rightarrow CO + 2H_2O \tag{1}$$

$$CO + 0.5O_2 \rightarrow CO_2 \tag{2}$$

$$H_2 + 0.5O_2 \rightarrow H_2O \quad (3)$$

The maximum temperature of the whole combustion region was monitored during the simulation, and the results were considered to have converged to a steady state when the maximum temperature was basically stable and the residual curves of the chemical component equation, momentum equation, energy equation and continuity equation converge to 10^{-4}, 10^{-6}, 10^{-6} and 10^{-6}, respectively.

2.2. Computational Conditions

The "V-type" waste incinerator burns 750 tons of MSW per day, with a grating length and width of 9.2 m and 14.4 m, respectively. The mesh model of the incinerator was established by using the Gambit software, comprising 1.98 million grid cells, as shown in Figure 3. In the modeling, the more complex structure of the grate furnace was reasonably simplified, ignoring the connection of various parts of the grate furnace, and simplifying the grate furnace feed opening and slag discharge opening as the wall surface. In the mesh drawing, the local areas with large changes in parameters such as secondary air vents were encrypted, and a high-quality hexahedral mesh was used for meshing. The grid quality check result is shown in Figure 3. It can be seen that 99% of the grid has a skewness of 0–0.25, an aspect ratio of 1–2.6, a cell volume of 0–0.003, and a neighboring cell size ratio of 0–2.01; the minimum mesh quality was 0.4, so the mesh quality can be considered good. The air was divided into two parts: primary and secondary air. The primary and secondary air volumes were 57,970.8 Nm^3/h and 23,500.3 m^3/h, and their temperatures were 410 K and 464 K, respectively.

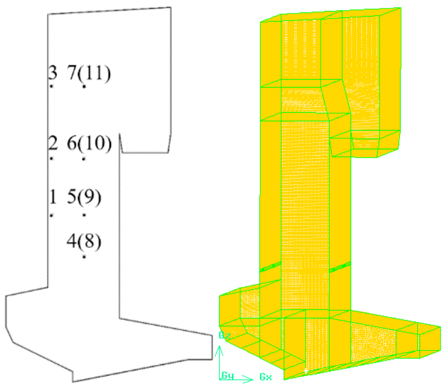

Figure 3. Measuring point position and mesh division.

2.3. Grid Independence Verification

This grid independence test simulation uses three groups of grids with 1.6 million, 1.92 million and 2.23 million grids, respectively. Figure 4 shows the variation curve of the average temperature of different height sections of the furnace chamber with the number of grids. From the figure, it can be seen that the temperature deviation of the three sets of grids was small, and so it can be considered that the numerical simulation results were independent of the number of grids. Therefore, considering the requirements of calculation accuracy and calculation time, we finally chose 1.92 million grids for calculation.

2.4. Model Reliability Verification

To verify the reliability of the model, a comparison between the simulated and measured temperatures of the 11 points of the first flue, as depicted in Figure 3, was presented in Figure 5. It can be seen that the simulated temperature was in good agreement with the measured temperature, with a relative error of less than 10%. Therefore, the employed model was reliable and can reasonably simulate the combustion of MSW.

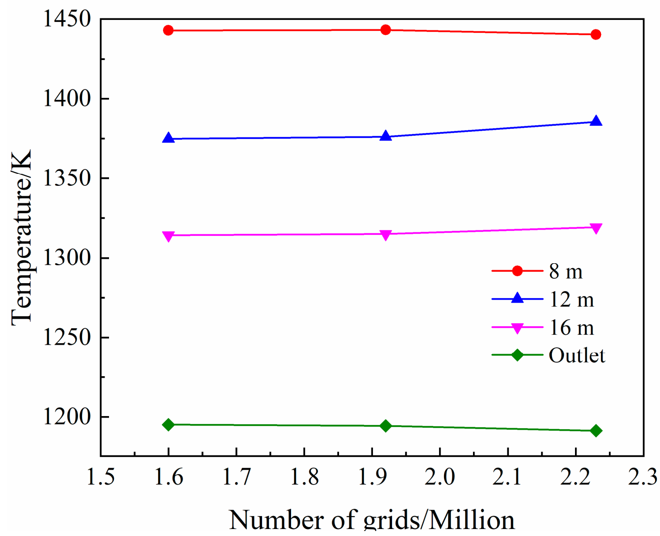

Figure 4. Variation curve of the average temperature of different height sections of the furnace chamber with the number of grids.

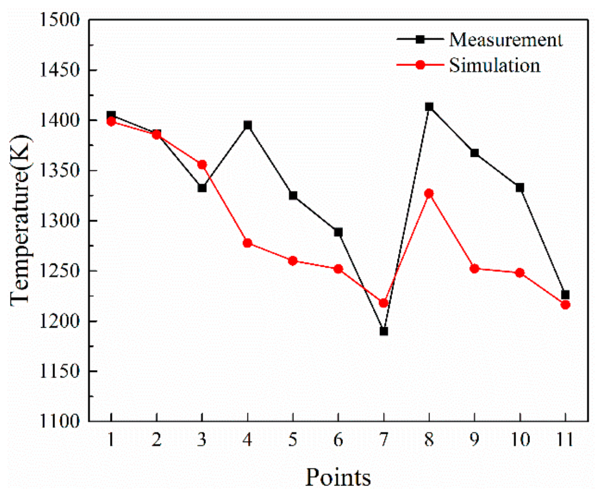

Figure 5. Measured and simulated temperatures.

2.5. Materials

MSW and ash were obtained from a waste incineration plant in Hubei province, China. Table 1 lists the results of the proximate and ultimate analyses (on an as received basis) of the MSW. Samples of cyclone separator ash, horizontal flue ash, bag filter ash, and slag (No. A1, A2, A3, and S1) were collected every 2 h on the same day. A schematic diagram of the sampling location was shown in Figure 6. The particle size distribution of the fly ash was analyzed by using a laser particle size analyzer. A scanning electron microscope (SEM) was used to analyze the microstructures of the fly ash and slag. X-ray fluorescence spectrometry (XRF) and X-ray diffraction (XRD) were used to analyze the components of the fly ash and slag. Figure 6 shows the sampling locations.

Table 1. Proximate and ultimate analyses (as received basis) of the MSW (wt%).

Moisture	Volatiles	Fixed Carbon	Ash	C	H	O	N	S	Cl	LHVnet, ar (kJ/kg)
55.48	24.91	11.25	8.36	21.79	2.47	10.53	0.87	0.17	0.33	7200

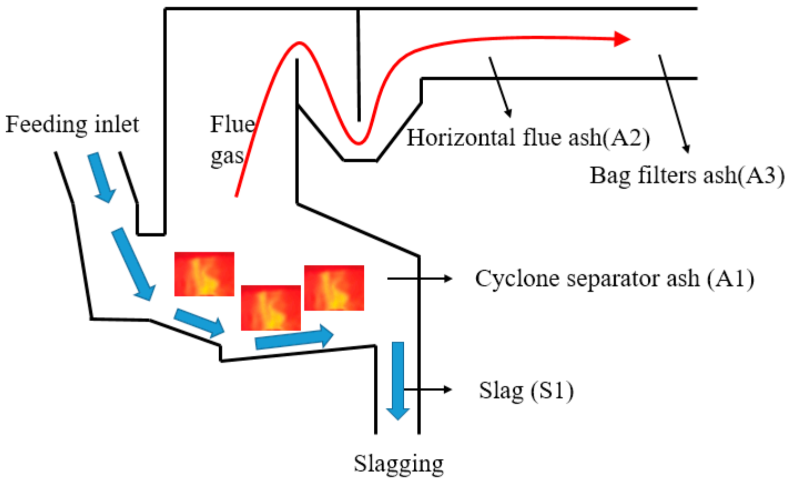

Figure 6. Schematic diagram of the sampling location.

3. Results

3.1. Combustion Simulation Results

Figure 7 shows the temperature distribution on the middle plane of the incinerator obtained through the simulation calculation. Since a large amount of secondary air is shot from the middle of the furnace, providing sufficient O_2, the combustible components appear in the middle of the furnace for secondary combustion, which is the main reason for the higher temperature in the middle and upper part of the furnace, with the highest temperature reaching 1650 K. In addition, the flue gas flows and mixes in the upper part of the incinerator. The flue gas then flows and mixes in the upper part of the furnace chamber and transfers heat to the water wall, so the flue gas temperature gradually decreases and tends to be uniform. Compared with Ref. [10], it was found that because the temperature of the primary air and the secondary air were lower than the temperature in the literature, the resulting maximum flame temperature was also lower, which is consistent with the general trend in the literature.

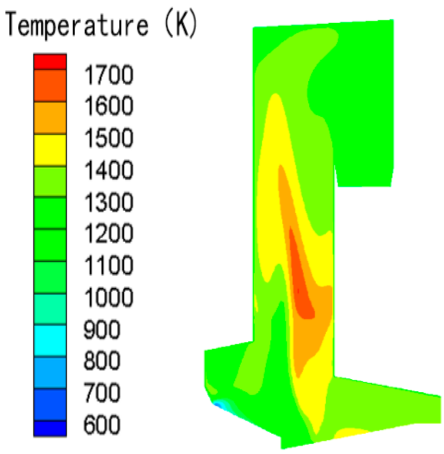

Figure 7. Temperature on the middle plane.

To provide a deeper insight, Figure 8 shows the simulated results of the combustion parameters along the bed length. At 0.38 m in the bed length direction, the gas temperature rose sharply because the volatile components started to precipitate and burn due to the joint radiative heating effect of the primary air and the furnace flue gas. The release rate of volatiles reached a peak at 4.15 m. After that, the gas temperature above the bed decreased due to the incomplete combustion caused by the large amount of volatiles precipitating and absorbing heat, as well as the decrease in oxygen concentration. After 4.6 m, the volatiles were almost completely precipitated. After 0.6 m, the fixed carbon started to burn, and with the increase of flue gas temperature, the burning rate of fixed carbon increased. By 4.15 m or so, the burning rate of coke slowed down, and after 4.2 m, the burning rate of fixed carbon increased significantly due to the violent burning bed temperature of volatile fraction. After the volatile fraction is completely precipitated, the gas temperature above the bed continued to rise under the effect of coke combustion, and the highest gas temperature above the bed reached 1450 K. After 5.67 m, the fixed carbon was basically burned completely, and the gas temperature above the bed gradually decreased with the burning of fixed carbon. As illustrated in Figure 6, the volatile release, fixed carbon combustion, and oxygen consumption in the first and third sections were almost the same. In comparison, the release of volatiles and the combustion of fixed carbon in the second section were completed earlier. In addition, the maximum burning rate of fixed carbon and the maximum release rate of volatile in the second part were lower than the other two parts, so the temperature of the second part was slightly lower.

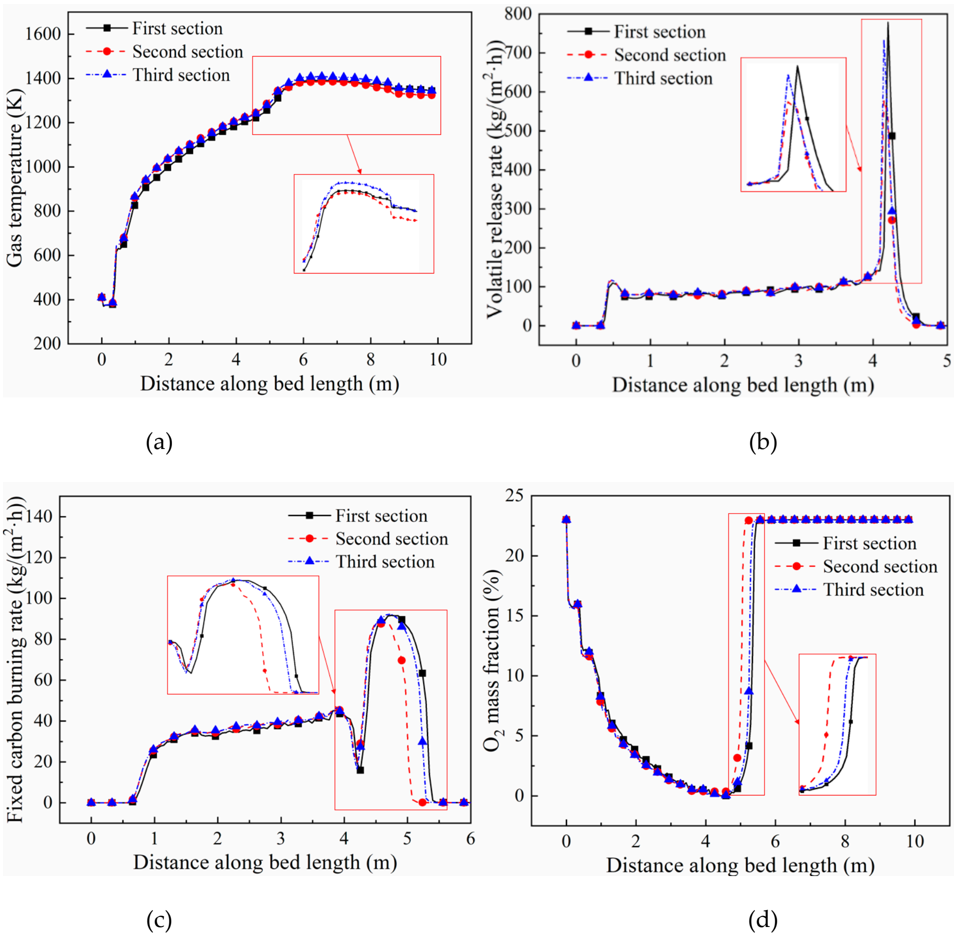

Figure 8. Combustion parameters along the bed length: (**a**) Variation of gas temperature along the length of the bed; (**b**) Variation of volatile release rate along the length of the bed; (**c**) Variation of fixed carbon burning rate along the length of the bed; (**d**) Variation of O_2 mass fraction along the length of the bed.

3.2. Particle Size Distribution of Fly Ash

Figure 9 shows the particle size distribution of the fly ash. The particle size range of the three types of fly ash was 0.01–1000 µm. Particle sizes less than 0.2 µm in A1 were almost zero, and the main particle size range was 15.8–100.2 µm. In A2, fly ash particles with a size of less than 148.3 µm accounted for 50% of the distribution, and fly ash particles with a size of less than 391.6 µm accounted for 90%. Particles smaller than 37.586 µm accounted for 50% of A3, with the main particle sizes ranging from 22.440 μm to 89.337 μm. Sample A3 is the fly ash collected from the last-stage bag filters. A comparison between the results of samples A2 and A3 shows that large-size ash particles were effectively captured by the bag filter.

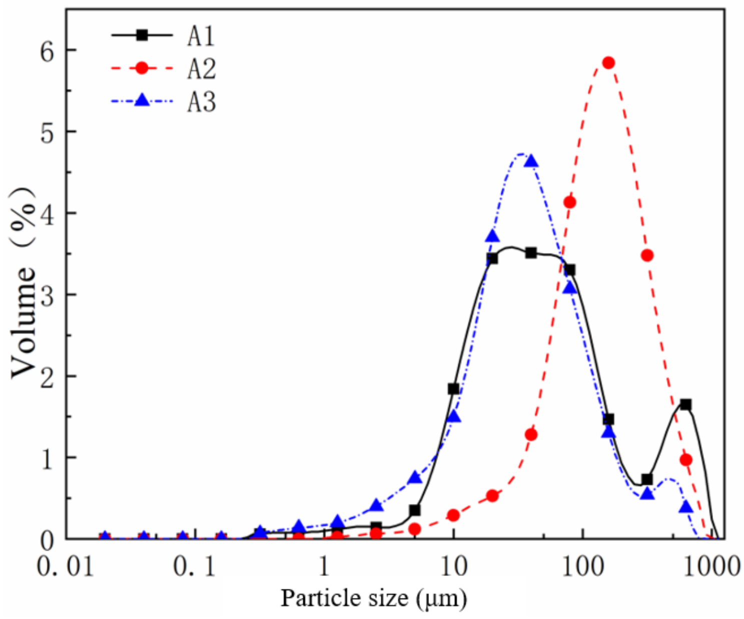

Figure 9. Particle size distribution of fly ash.

3.3. XRF and XRD Analysis of Fly Ash

Table 2 shows the main chemical compositions of the incineration ash and slag. The main oxides of samples A1, A2, and S1 were CaO and SiO_2, accounting for more than 50% of the total. The minor components were MgO, Al_2O_3, Fe_2O_3, etc. The main oxide of sample A3 was CaO, and the minor components were Na_2O and K_2O. Excessive lime was sprayed to remove acidic gas, resulting in a significant increase in the CaO content of sample A3. According to the simulation results, the maximum temperature in the furnace reached 1500 K. Therefore, the low-boiling-point heavy metal (such as Zn) content was higher in the fly ash. The MSW contained plastic products, kitchen waste, etc., which contain more Cl. Chlorides readily volatilize into the flue gas and adsorb onto the surface of fly ash, resulting in a higher content of Cl in the fly ash.

Table 2. Main composition of MSW incineration ash and slag (wt%).

Composition	A1	A2	A3	S1	Composition	A1	A2	A3	S1
CaO	36.71	34.81	60.75	28.28	K_2O	1.77	2.70	6.35	2.05
SiO_2	27.33	20.52	4.89	36.67	P_2O_5	3.11	2.66	0.62	4.36
MgO	8.10	5.66	1.43	4.74	TiO_2	1.61	1.84	0.35	1.36
Al_2O_3	8.10	6.42	1.17	8.60	ZnO	0.46	0.80	0.97	0.32
Cl	4.690	6.956	23.347	2.828	BaO	0.22	0.22	0.07	-
Fe_2O_3	4.23	4.87	0.88	4.57	MnO	0.14	0.15	0.03	0.14
SO_3	5.35	14.10	10.80	5.09	CuO	0.09	0.07	0.12	0.07
Na_2O	2.53	4.84	11.12	3.37	PbO	0.04	0.06	0.28	0.02

The waste incineration ash and slag were also analyzed by XRD, and the results are shown in Figure 10. Waste incineration ash and slag are mainly composed of metal oxides and non-metal oxides. The main components of A1 and A2 are SiO_2, CaO, $CaCO_3$, and $CaSO_4$. A3 is treated with lime water; the main components of A3 were $Ca(OH)_2$ and metal chlorides. The components of S1 are relatively simple and mainly contain SiO_2 and Fe_2O_3.

Comparing the XRD results in literature Ref. [25], it can be seen that the basic components were roughly the same, while the amounts of NaCl and KCl were significantly higher. This is because stabilizers such as coal fly ash are added to MSW fly ash.

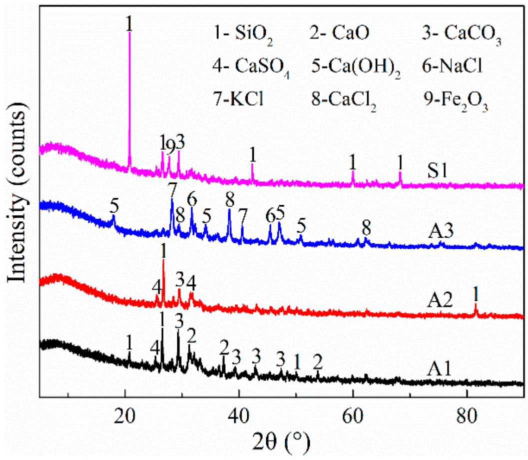

Figure 10. XRD of waste incineration in ash and slag.

3.4. Incineration Ash and Slag Microscopic Morphology

Figure 11 shows the SEM images of the waste incineration ash; the fly ash samples mainly contained irregularly shaped particles and spherical and elliptical particles. We have estimated the particle size of the incineration ash in Figure 11, and the particle sizes of A1, A2, A3 and S1 were about 40 µm, 72 µm, 56 µm and 18 µm, respectively. The slag sample (S1) mainly contained irregularly shaped particles, and there were many pores on the surface of the particles. It can also be observed that the particles in the A1 sample were smaller and more compact. In contrast, the structure of the particles of samples A2, A3, and S1 appeared looser. In addition, the large particles of sample A3 adsorbed a large number of very small particles on the surface. This is due to the fact that the particles of sample A3 contained more alkali metals such as Na and Ca, as shown in Table 2.

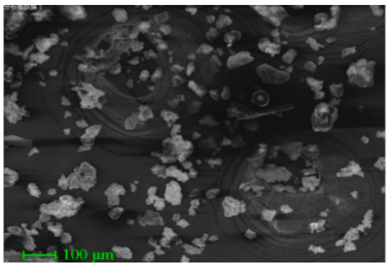

(a1) A1(×300)

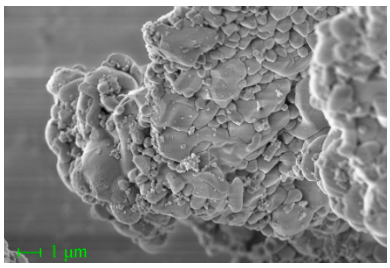

(a2) A1(×1300)

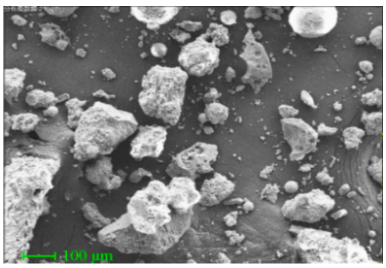

(b1) A2(×300)

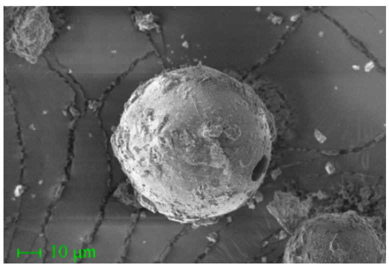

(b2) A2(×1000)

Figure 11. *Cont.*

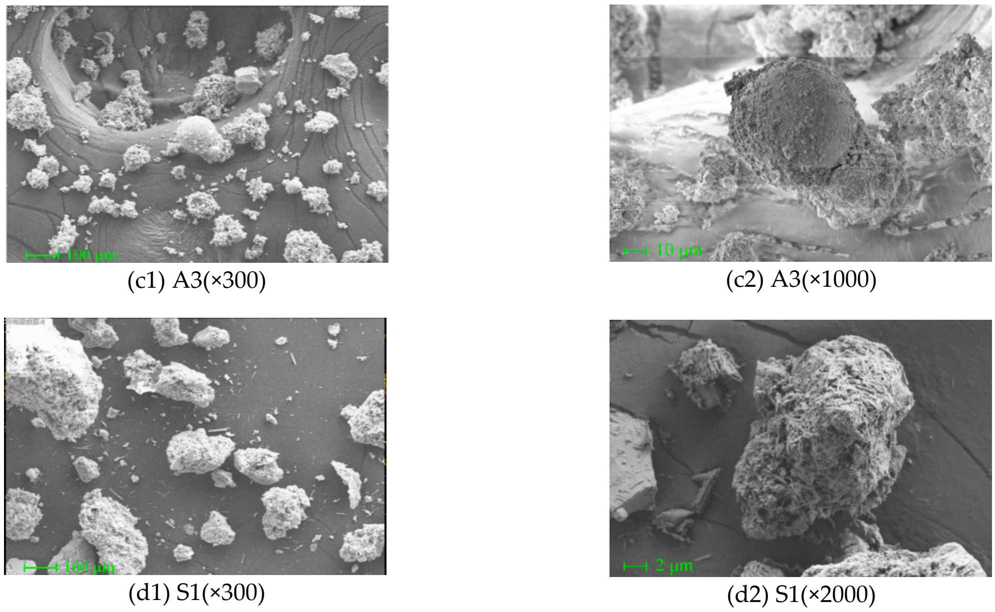

Figure 11. SEM of waste incineration ash and slag: (**a1**) SEM image of the cyclone separator ash at 300x magnification; (**a2**) SEM image of the cyclone separator ash at 1300x magnification; (**b1**) SEM image of the horizontal flue ash at 300x magnification; (**b2**) SEM image of the horizontal flue ash at 1000x magnification; (**c1**) SEM image of the bag filters ash at 300x magnification; (**c2**) SEM image of the bag filters ash at 1000x magnification; (**d1**) SEM image of the slag at 300x magnification; (**d2**) SEM image of the slag at 2000x magnification.

4. Conclusions

In this paper, the combustion process of MSW in a "V-shaped" waste incinerator was investigated using CFD software, and the characteristics of fly ash and slag were analyzed using a laser particle analyzer, scanning electron microscope (SEM), X-ray fluorescence spectrometry (XRF) and X-ray diffraction (XRD). The analysis of the results of the combustion simulations and the related images led to several conclusions:

(1) The simulation method and model proposed in this paper are able to simulate the incineration process of a V-type waste incinerator, and the simulated temperature results are within a 10% error of the actual measured temperature. Therefore, the employed model is reliable and can reasonably simulate the combustion of MSW.

(2) In the combustion process of MSW, the combustion of volatiles and fixed carbon is mainly concentrated in the middle part of the grate. When secondary air is fed into the furnace chamber, volatiles are burned in the middle of the chamber, forming a high temperature zone with a maximum temperature of about 1650 K.

(3) The particle size of fly ash along the incineration process is less than 1000 μm, and the main particle size range of fly ash captured by the bag filter is between 17.8–89.3 μm, which has a high capture efficiency. The waste incineration fly ash mainly contains irregularly shaped agglomerated particles, as well as spherical or ellipsoidal particles. The surface of the particles is uneven, and small flat, flocculent particles are adhered to the surface.

(4) There are some differences in the main components of incineration ash and slag along the combustion process. The main oxide components in cyclone separator, horizontal flue fly ash and slag are CaO and SiO_2, secondary components are MgO, Al_2O_3, Fe_2O_3, etc. The main constituent elements are O, Ca, Si, Cl, Mg, Al, etc. The bag dust fly ash is mainly CaO, the secondary components are Na_2O and K_2O, and the main constituent elements are Ca and Cl. Heavy metal elements such as Pb, Cu, Zn, Cr, etc., are present in waste incineration ash and slag.

Author Contributions: Project administration, Z.L. (Zixue Luo); Investigation, W.C.; Resources, X.Y., Z.L. (Zhigang Li) and J.Y.; Writing—original draft, Y.W. and Q.C.; Writing—review and editing, Z.L. (Zixue Luo). All authors have read and agreed to the published version of the manuscript.

Funding: This research was funded by the National Key R&D Program of China (2019YFC1904003) and the National Science Foundation of China (No. 51776078).

Data Availability Statement: All data, models, and code generated or used during the study appear in the submitted article.

Conflicts of Interest: The authors declare no conflict of interest in publishing this result.

Nomenclature

A1	cyclone separator ash
A2	horizontal flue ash
A3	bag filters ash
S1	slag

References

1. Wiśniewska, M.; Kulig, A.; Lelicińska-Serafin, K. Odour Nuisance at Municipal Waste Biogas Plants and the Effect of Feedstock Modification on the Circular Economy—A Review. *Energies* **2021**, *14*, 6470. [CrossRef]
2. Jing, Z.; Fan, X.; Zhou, L.; Fan, J.; Zhang, Y.; Pan, X.; Ishida, E.H. Hydrothermal solidification behavior of municipal solid waste incineration bottom ash without any additives. *Waste Manag.* **2013**, *33*, 1182–1189. [CrossRef]
3. Shareefdeen, Z.; Elkamel, A.; Tse, S. Review of current technologies used in municipal solid waste-to-energy facilities in Canada. *Clean Technol. Environ. Policy* **2015**, *17*, 1837–1846. [CrossRef]
4. Zhao, X.G.; Jiang, G.W.; Li, A.; Li, Y. Technology, cost, a performance of waste-to-energy incineration industry in China. *Renew. Sustain. Energy Rev.* **2016**, *55*, 115–130.
5. Kanhar, A.H.; Chen, S.; Wang, F. Incineration Fly Ash and Its Treatment to Possible Utilization: A Review. *Energies* **2020**, *13*, 6681. [CrossRef]
6. Chen, X.; Geng, Y.; Fujita, T.J.W.M. An overview of municipal solid waste management in China. *Waste Manag.* **2010**, *30*, 716–724. [CrossRef]
7. Bermúdez, C.A.; Porteiro, J.; Varela, L.G.; Chapela, S.; Patiño, D.J.F.P.T. Three-dimensional CFD simulation of a large-scale grate-fired biomass furnace. *Fuel Process. Technol.* **2020**, *198*, 106219. [CrossRef]
8. Karim, M.R.; Bhuiyan, A.A.; Naser, J.J.R.E. CFD simulation of biomass thermal conversion under air/oxy-fuel conditions in a reciprocating grate boiler. *Renew. Energy* **2020**, *146*, 1416–1428. [CrossRef]
9. Yang, Y.B.; Swithenbank, J.J.W.M. Mathematical modelling of particle mixing effect on the combustion of municipal solid wastes in a packed-bed furnace. *Waste Manag.* **2008**, *28*, 1290–1300. [CrossRef]
10. Yan, M.; Wang, J.; Hantoko, D.; Kanchanatip, E.J.F. Numerical investigation of MSW combustion influenced by air preheating in a full-scale moving grate incinerator. *Fuel* **2021**, *285*, 119193. [CrossRef]
11. Xu, J.; Liao, Y.; Yu, Z.; Cai, Z.; Ma, X.; Dai, M.; Fang, S.J.F. Co-combustion of paper sludge in a 750 t/d waste incinerator and effect of sludge moisture content: A simulation study. *Fuel* **2018**, *217*, 617–625. [CrossRef]
12. Becidan, M.; Ditaranto, M.; Carlsson, P.; Bakken, J.; Olsen, M.N.P.; Stuen, J. Oxyfuel Combustion of a Model MSW—An Experimental Study. *Energies* **2021**, *14*, 5297. [CrossRef]
13. Shishkin, A.A.; Shishkin, A.A.; Dushkina, N.N. Research of the removal of fly ash particles from industrial boiler flue gases. *Int. J. Energy Clean Environ.* **2019**, *20*, 273–289. [CrossRef]
14. Huang, T.; Liu, L.; Zhou, L.; Yang, K.J.C. Operating optimization for the heavy metal removal from the municipal solid waste incineration fly ashes in the three-dimensional electrokinetics. *Chemosphere* **2018**, *204*, 294–302. [CrossRef] [PubMed]
15. Lin, H.; Ma, X.J.W.M. Simulation of co-incineration of sewage sludge with municipal solid waste in a grate furnace incinerator. *Waste Manag.* **2012**, *32*, 561–567. [CrossRef]
16. Yang, Y.B.; Newman, R.; Sharifi, V.; Swithenbank, J.; Ariss, J.J.F. Mathematical modelling of straw combustion in a 38 MWe power plant furnace and effect of operating conditions. *Fuel* **2007**, *86*, 129–142. [CrossRef]
17. Liang, Z.; Ma, X.J.W.M. Mathematical modeling of MSW combustion and SNCR in a full-scale municipal incinerator and effects of grate speed and oxygen-enriched atmospheres on operating conditions. *Waste Manag.* **2010**, *30*, 2520–2529. [CrossRef]
18. Hu, Z.; Jiang, E.; Ma, X.Q. Numerical simulation on NOX emissions in a municipal solid waste incinerator. *J. Clean. Prod.* **2019**, *233*, 650–664. [CrossRef]
19. Goh, Y.; Lim, C.; Zakaria, R.; Chan, K.; Reynolds, G.; Yang, Y.; Siddall, R.; Nasserzadeh, V.; Swithenbank, J.J.P.S.; Protection, E. Mixing, modelling and measurements of incinerator bed combustion. *Process. Saf. Environ. Prot.* **2000**, *78*, 21–32. [CrossRef]
20. Yang, Y.; Ryu, C.; Goodfellow, J.; Sharifi, V.N.; Swithenbank, J. Modelling waste combustion in grate furnaces. *Process Saf. Environ. Prot.* **2004**, *82*, 208–222. [CrossRef]

21. Zhou, L.; Bai, L.; Zhang, L.; Shi, W.; Agarwal, R.K. Validation and Comparison of Discrete Element Model and Two-Fluid Model for Dense Gas-Solid Flow Simulation in a Fluidized Bed. *Int. J. Energy Clean Environ.* **2019**, *20*, 135–151. [CrossRef]
22. Cellek, M.S. Evaluation of oxygen enrichment effects on distribution combustion mode in a laboratory-scale furnace. *Int. J. Energy Clean Environ.* **2022**, *23*, 19–37. [CrossRef]
23. Sigal, A.; Safiants, A.S.; Magera, Y.M. Diagnostic system for predicting the composition of municipal solid waste burnt in the recovery boiler. *Int. J. Energy Clean Environ.* **2017**, *18*, 175–187.
24. Kolibaba, O.B.; Sokolskiy, A.I.; Gabitov, R.N. Research of the pyrolysis of municipal solid waste aimed at improving the efficiency of thermal reactors. *Int. J. Energy Clean Environ.* **2017**, *18*, 147–160. [CrossRef]
25. Masashi, K.; Takeshi, K.; Youichi, S. MSW fly ash stabilized with coal ash for geotechnical application. *J. Hazard. Mater.* **2000**, *76*, 265–283.